

Optical and structural properties of sol gel derived materials embedded in porous anodic alumina

N.V. Gaponenko ^{a,*}, I.S. Molchan ^a, D.A. Tsyrcunov ^a, G.K. Maliarevich ^a,
M. Aegerter ^b, J. Puetz ^b, N. Al-Dahoudi ^b, J. Misiewicz ^c, R. Kudrawiec ^c,
V. Lambertini ^d, N. Li Pira ^d, P. Repetto ^d

^a *Belarusian State University of Informatics and Radioelectronics, P. Browki St.6, 220013 Minsk, Belarus*

^b *Leibniz Institut fuer Neue Materialien , Department of Coating Technology, D 66123, Saarbruecken, Germany*

^c *Institute of Physics, Wroclaw University of Technology, Wybrzeze, Wyspianskiego 27, 50 370 Wroclaw, Poland*

^d *Centro Ricerche FIAT Optics and Photonics, Strada Torino, 50 10043 Orbassano (TO), Italy*

Available online 7 April 2005

Abstract

Structures comprising a xerogel, doped with lanthanide ions (erbium, terbium and europium), embedded in porous anodic alumina (PAA) have been fabricated and their optical and electrical characteristics have been studied. Erbium photoluminescence at 1.53 μm from titania xerogel/PAA was found to increase with the number of xerogel layers and erbium concentration for the excitation wavelength 532 nm, matching the area of transparency of both titania xerogel and PAA. Visible green and red electroluminescence was observed for terbium and europium doped In_2O_3 and SnO_2 xerogels embedded in porous anodic alumina. The improvement of the electrical properties of the xerogel/PAA cell is discussed, taking into account the observed ability of conducting $\text{In}_2\text{O}_3:\text{Sn}$ (ITO) nanoparticles to penetrate into the anodic alumina pores.

Keywords: Erbium; Terbium; Europium; Luminescence; Porous anodic alumina

1. Introduction

Porous anodic alumina films are of considerable interest due to their cellular structure, with regularly arranged mesoscopic channels of the pores [1,2]. Such structures can be used as hosts for sol gel films, which often give new properties to

* Corresponding author. Tel.: +375 172 39 88 69; fax: +375 172 31 09 14.

E mail address: nik@nano.bsuir.edu.by (N.V. Gaponenko).

these materials. This was shown for the enhanced photoluminescence of erbium, terbium and europium from titania, silica and alumina xerogels embedded in porous anodic alumina of 1–30 μm thickness [3–5].

A promising field of application of lanthanide-doped xerogels is for electroluminescent devices, which are currently the focus of substantial research effort due to potential use in flat panel displays, light emitting diodes, lasers, etc. Most of the work in this area is directed to the synthesis of organic EL materials, and high luminous efficiencies at low operational voltages have been demonstrated [6]. However, organic compounds generally have a number of disadvantages, including poor thermal and mechanical stability, resulting in the occurrence of current voltage instability [7,8].

In this context, it is of interest to use oxide-based lanthanide-doped materials that may be synthesized by simpler methods, such as electrochemical deposition [9] and sol gel synthesis [10,11], which offer improved stability. An additional benefit of study of porous anodic alumina as an electroluminescent cell also arises from the enhanced photoluminescence of lanthanides when embedded therein. Recent reports on the anisotropy of the photonic density of states in porous anodic alumina, with the maximum along the direction of the pore channels [12,13] render this material of interest as a template for electroluminescent structures. A further attractive feature of lanthanide luminescence in xerogels is the low concentration quenching reported for terbium- and europium-doped xerogel/PAA structures [14,15]. Recently, titania was considered as a good host for optically active trivalent erbium ions, exhibiting a strong photoluminescence at 1.53 μm [16–18].

In this work, the possibility of increasing the erbium photoluminescence in xerogel/porous anodic alumina structure is considered, along with prospective application of the structure for electroluminescent devices. Terbium and europium electroluminescence (EL) in SnO_2 and In_2O_3 xerogels embedded in porous anodic alumina is reported, with the route to assuring electrical contact between the xerogel and the transparent electrode, using a suspension of conducting ITO nanoparticles, is discussed.

2. Experimental

Several sol gel derived coatings were used. One group comprises In_2O_3 or SnO_2 xerogel films fabricated from diluted colloidal solutions of $\text{Sn}(\text{OH})_2$ or $\text{In}(\text{OH})_3$ that were prepared from tin or indium chloride precursors, accordingly. In order to improve the conductivity of the xerogels, a further group of ITO-xerogel films was fabricated from these solutions using Sn/In ratio in xerogel ranging from 4 to 14 mol%. Titanium dioxide films were prepared from $\text{Ti}(\text{OC}_2\text{H}_5)_4$ precursor, (see [16] for details). These solutions were mixed with nitrates of lanthanide ions to achieve 30–60 wt% Er_2O_3 , Tb_2O_3 or Eu_2O_3 in the respective xerogel films.

The last group of coatings, comprising ITO nanoparticles, was fabricated using a suspension of ITO nanoparticles [19].

The films were fabricated by spinning the individual solutions either on wafers of fused silica, or thermally oxidized silicon with 0.1 μm thick silicon dioxide or films of PAA. The typical thicknesses of ITO-xerogel film and ITO-film derived from suspension and deposited by spinning on flat surfaces were 0.01 and 0.5 μm , respectively.

PAA films, 5 and 15 μm thick, with a pore diameter of 90 nm, were fabricated by anodizing of an aluminum layer deposited by magnetron sputtering onto silicon substrates; anodizing was carried out at a constant current density of 5.5 mA/cm^2 in 1.2 M H_3PO_4 . Additionally, selected samples were etched to achieve increased pore diameters. Fig. 1 shows a typical image of such a porous film. To obtain terbium- or europium-related electroluminescence, the sols containing lanthanide ions were deposited onto PAA by spinning at 2700 rpm for 30 s followed by a thermal treatment. An ITO electrode sputtered onto glass surface was mechanically pressed on the top surface of PAA filled with xerogel (Fig. 2), with the silicon substrate serving as the second electrode.

Room-temperature, 1.53 μm infrared emission was studied for titania xerogels containing 30 and 60 wt% of Er_2O_3 fabricated by spinning on a porous anodic alumina. Excitation was performed with an argon laser, operating at 300 or 532 nm.

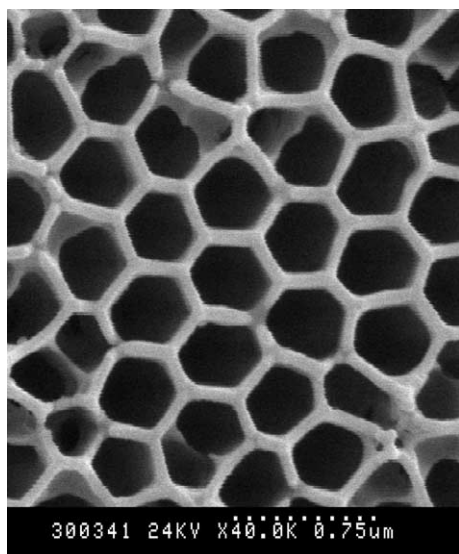


Fig. 1. SEM image of porous anodic alumina film (plane view) fabricated at constant current density of 5.5 mA/cm^2 in $1.2 \text{ M H}_3\text{PO}_4$ electrolyte.

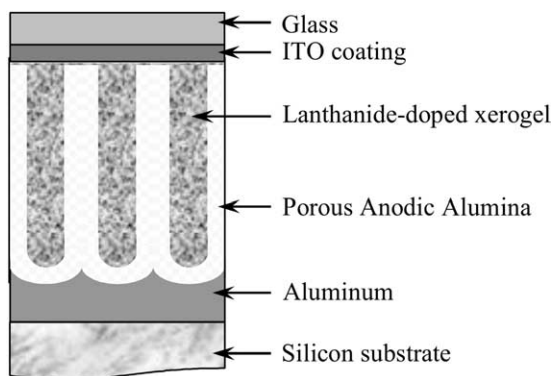


Fig. 2. Schematic view of EL cell comprising xerogel/porous anodic alumina structure, fabricated on silicon. The structure reveals visible Eu or Tb related luminescence when positive potential above 40 or 90 V is applied to the ITO electrode for Eu or Tb doped In_2O_3 and SnO_2 xerogels, respectively.

3. Results and discussion

3.1. $1.53 \mu\text{m}$ Infrared emission

Erbium-doped titania xerogel films, fabricated on PAA, reveal strong room-temperature PL at $1.53 \mu\text{m}$, which is associated with the ${}^4\text{I}_{13/2} \rightarrow$

${}^4\text{I}_{15/2}$ transition of Er^{3+} in the titania xerogel (Fig. 3). Depending on the excitation wavelength, the erbium PL increases or decreases with the number of deposited xerogel layers. Particularly it increases for the 532 nm excitation wavelength (Fig. 3(a)) and decreases for the 300 nm wavelength. Erbium PL increases also with the increase of Er_2O_3 concentration in the titania xerogel from 30 to 60 wt% (Fig. 3(c)). The observed behaviour of the erbium PL intensity with the number of xerogel layers for these two excitation wavelengths can be understood by considering the earlier transmittance measurements of titania xerogel and porous anodic alumina [20]. Contrary to the 300 nm excitation wavelength, both the titania xerogel and the porous anodic alumina reveal a higher transparency for the 532 nm excitation wavelength, providing favourable conditions for light propagation at 532 nm and $1.53 \mu\text{m}$. Thus, an increase in the titania xerogel content (amount of active luminescent centres) results in an increase of the erbium PL intensity for the 532 nm excitation wavelength. It may be probable to increase further the $1.53 \mu\text{m}$ emission by increase of erbium concentration in xerogel and the number of xerogel layers. The samples do not reveal a strong concentration quenching of erbium photoluminescence unlike erbium-implanted semiconductors, and the transparency of titania at the excitation wavelength allows a further build up of the xerogel layers within the anodic alumina pores.

3.2. Electroluminescent cell

When a positive potential is applied to the ITO electrode for the structure of Fig. 2, the visible red (europium-doped xerogels) and green (terbium-doped xerogels) emission appears at applied voltages above 40 and 90 V for In_2O_3 and SnO_2 xerogels, respectively. The observed light emission from this structure is associated with the dominant optical transitions ${}^5\text{D}_0 \rightarrow {}^7\text{F}_2$ of Eu^{3+} at 617 nm and ${}^5\text{D}_4 \rightarrow {}^7\text{F}_5$ of Tb^{3+} at 545 nm in In_2O_3 and SnO_2 xerogels. Both of the fabricated structures, with PAA thicknesses of 5 and $15 \mu\text{m}$, exhibited visually similar intensities of emission.

The voltage current characteristics (VCC) of the EL structures are presented in Fig. 4. In_2O_3

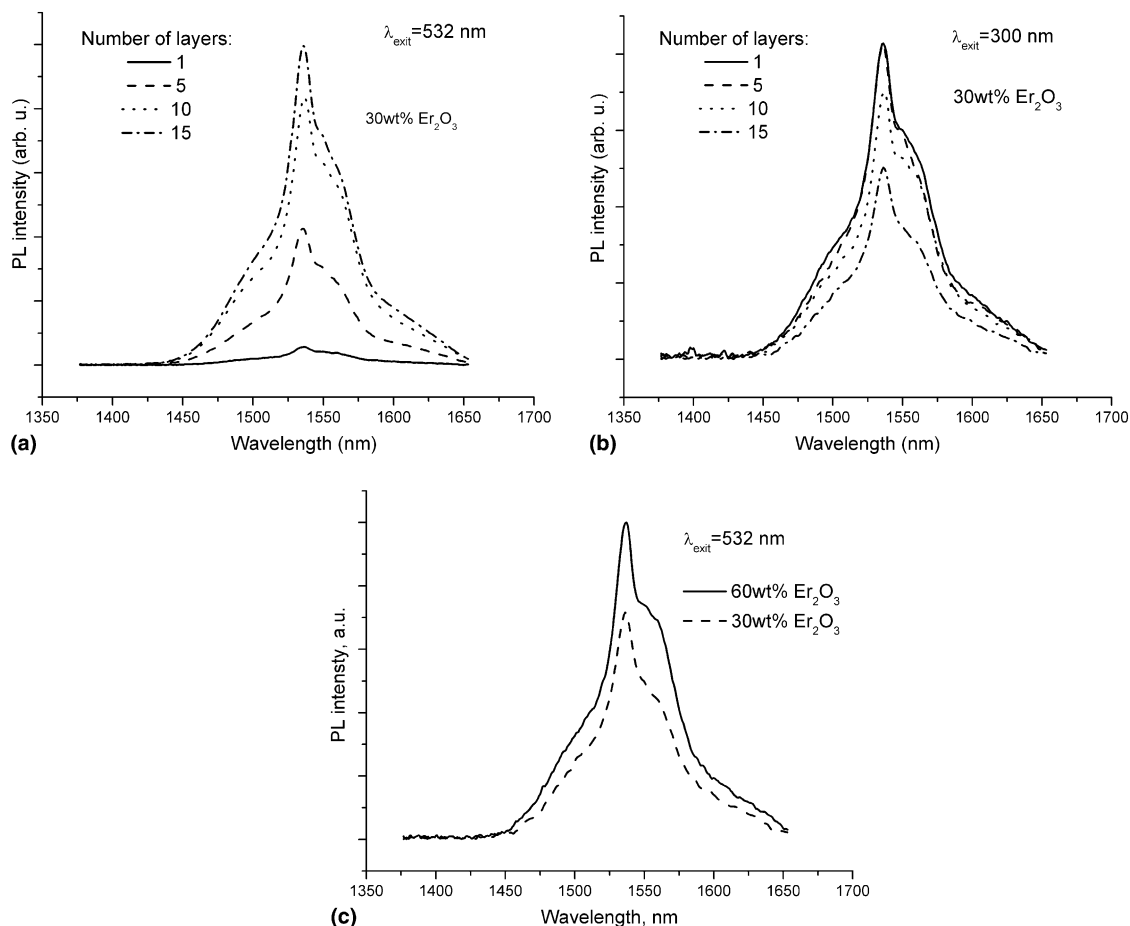


Fig. 3. PL spectra around 1.53 μm from erbium doped titania xerogels layers (30 and 60 wt% Er_2O_3) deposited by spinning from 1 to 15 times onto porous anodic alumina followed by annealing at 900 $^\circ\text{C}$ for 20 min.

xerogel based structures operate at lower voltages than that of SnO_2 . From the shape of the VCC, it is concluded that the EL mechanism involves a double injection (holes from the ITO layer and electrons from the bottom electrode) and a recombination of the carriers in the phosphor with a transfer of the energy to the lanthanide ions resulting in a photon emission.

Further lowering of the electrical resistance of the xerogel/porous anodic alumina structure can be achieved by: (i) ensuring more reliable electrical contact between the conductive xerogel and the upper conductive electrode and (ii) improving the conductivity of the xerogel material, doped with the lanthanide ions.

Ensuring electrical contact may be achieved by use of an additional conductive sublayer, this conductive sublayer could comprise ITO nanoparticles [19]. Typically, an 0.5 μm thick ITO-film, with a sheet resistance of about 500 Ω/\square can be obtained by spinning a suspension of ITO nanoparticles followed by annealing at 550 $^\circ\text{C}$.

The ability of the dispersed nanoparticles to penetrate through the channels of the anodic alumina pores was investigated with SEM, and the images reveal their penetration into the channels of the anodic alumina after simple spin deposition from dispersion (Fig. 5). The degree of pore filling increases by sequential deposition of spin-on layers from one to five. Further, the diffusion of the lan-

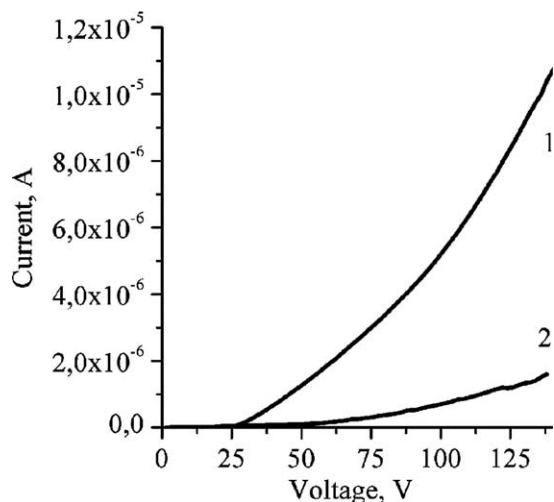


Fig. 4. Voltage current characteristics of EL structure fabricated on PAA of $15\ \mu\text{m}$ thick with Eu doped xerogel films: xerogel $\text{Eu}_2\text{O}_3\ \text{In}_2\text{O}_3$ (curve 1), $\text{Eu}_2\text{O}_3\ \text{SnO}_2$ (curve 2). Sample dimensions are $5 \times 5\ \text{mm}^2$.

thanide ions into the ITO-particles seems unfavourable. Examination of the structure fused silica/ITO-film/europium-or terbium-doped titania xerogel, subjected to a conventional furnace annealing at $1000\ ^\circ\text{C}$ for 12 h does not reveal diffusion of lantha-

nide ions into ITO nanoparticles. Furthermore, room-temperature measurements of the sheet resistivity, photoluminescence and photoluminescence excitation spectroscopy (PLE) do not confirm lanthanide diffusion as well. These structures exhibit PL and PLE spectra typical of terbium and europium in titania xerogels reported earlier [4,5].

In order to improve the conductivity of the xerogel material, several coatable solutions, with the Sn/In ratio in the ITO-xerogel ranging from 4 to 14 mol%, have been fabricated. The sheet resistance measurements of the corresponding ITO-xerogel spin-on films are presented in Table 1.

Table 1

Sheet resistance ($\text{k}\Omega/\square$) of ITO xerogel films fabricated on SiO_2/Si structure depending on the annealing temperature and the Sn/In ratio

Sn/In ratio (mol%)	Annealing temperature ($^\circ\text{C}$)					
	500	600	700	800	900	1000
4	>100	>100	>100	90	80	>100
8	45	35	60	97	75	25
10	30	25	30	45	80	>100
14	83	>100	>100	>100	>100	>100

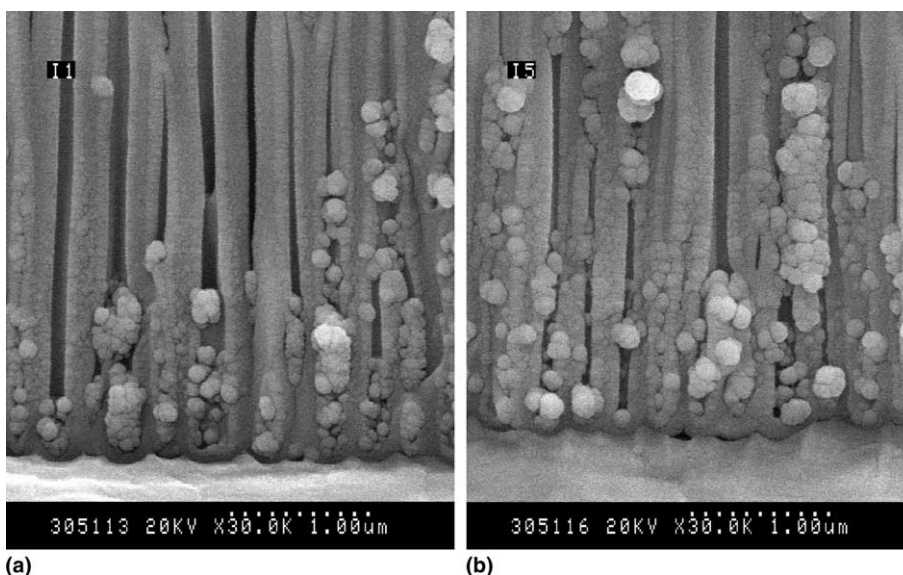


Fig. 5. SEM images of porous anodic alumina after one (a) and five (b) depositions of ITO nanoparticles fabricated by spinning from suspension.

The most conductive ITO-xerogel films were found with Sn/In ratio of 8 and 10 mol% subjected to thermal treatment at a temperature ranging from 500 to 700 °C. However, additional doping of these films with 30 wt% Eu_2O_3 results in a marked (two orders of magnitude) decrease of their conductivity.

Probably, other transparent conductive oxides such as ZnO:Al (AZO) [21], SnO_2 :Sb (ATO) [22], along with their moderate doping with lanthanide ions, could provide layers of lower resistivity. Their sol gel synthesis in porous anodic alumina may also further improve the electrical characteristics of the electroluminescent cell comprising the xerogel/porous anodic alumina structure.

4. Conclusions

Structures comprising lanthanide-doped (erbium, terbium and europium) xerogel/porous anodic alumina have been synthesized. Photoluminescence at 1.53 μm , by excitation at 532 nm of the erbium-doped titania xerogel increases with the erbium concentration and the number of xerogel layers. This excitation wavelength is optimum for the transparency of both the titania xerogel and porous anodic alumina.

Visible green and red electroluminescence, observed for terbium- and europium-doped In_2O_3 and SnO_2 xerogels embedded in porous anodic alumina, is reported. Advanced development of xerogel/porous anodic alumina structure is thought to arise from the observed ability of ITO nanoparticles to penetrate the anodic alumina pores. This can provide more reliable electrical contact between the conductive electrode and the conductive xerogels doped with the lanthanide ions. This effect and the influence of lanthanide ions on the conductivity of other conductive xerogel materials like ZnO:Al and SnO_2 :Sb and their possible synthesis in two-dimensional periodical porous anodic alumina cells will be addressed in subsequent papers.

Acknowledgements

This work was supported by INTAS (project 03-51-6486) and the International Science Techno-

logical Centre (project B-276.2). N.V. Gaponenko is also grateful to DAAD for supporting a research visit of the Leibniz Institut fuer Neue Materialien, Department of Coating Technology, Saarbruecken. Stimulating discussion with Prof. G.E. Thompson (The University of Manchester) and technical assistance of Dr. E.A. Stepanova (Belarusian State University of Informatics and Radioelectronics) in sol gel synthesis are gratefully acknowledged.

References

- [1] G.E. Thompson, R.C. Furneaux, G.C. Wood, J.A. Richardson, J.S. Goode, *Nature* 272 (1978) 433.
- [2] V.P. Parkhutik, V.I. Shershulsky, *J. Phys. D* 25 (1992) 1258.
- [3] N.V. Gaponenko, V.M. Parkun, O.S. Katernoga, V.E. Borisenko, A.V. Mudryi, E.A. Stepanova, A.I. Ratko, M. Cavanagh, B. O'Kelly, J.F. McGilp, *Thin Solid Films* 297 (1997) 202.
- [4] N.V. Gaponenko, J.A. Davidson, B. Hamilton, P. Skeldon, G.E. Thompson, X. Zhou, J.C. Pivin, *Appl. Phys. Lett.* 76 (2000) 1006.
- [5] N.V. Gaponenko, I.S. Molchan, G.E. Thompson, P. Skeldon, A. Pakes, R. Kudrawiec, L. Bryja, J. Misiewicz, *Sensor. Actuator. A* 99 (2002) 71.
- [6] X. Zhou, M. Pfeffer, J. Blochwitz, A. Werner, A. Nollau, T. Fritz, K. Leo, *Appl. Phys. Lett.* 78 (2001) 412.
- [7] E.A. Lebedev, M.Ja. Goikhman, K.D. Tsendin, I.V. Podeshvo, E.I. Terukov, V.V. Kudrjavitsev, *Semiconductors* 38 (2004) 1078.
- [8] N.A. Poklonski, E.F. Kislyakov, D.I. Sagadak, A.I. Siaglo, G.G. Fedoruk, *Tech. Phys. Lett.* 27 (2001) 180.
- [9] H.A. Lopez, P.M. Fauchet, *Phys. Status Solidi A* 182 (2000) 413.
- [10] A. Moadhen, H. Elhouichet, S. Romdhane, M. Oueslati, J.A. Roger, H. Bouchriha, *Semicond. Sci. Tech.* 18 (2003) 703.
- [11] H. Elhouichet, A. Moadhen, M. Ferid, M. Oueslati, B. Canut, J.A. Roger, *Phys. Status Solidi A* 197 (2003) 350.
- [12] N.V. Gaponenko, I.S. Molchan, A.A. Lutich, S.V. Gaponenko, *Solid State Phenom.* 97 98 (2004) 251.
- [13] A.A. Lutich, S.V. Gaponenko, N.V. Gaponenko, I.S. Molchan, V.A. Sokol, V. Parkhutik, *Nano Lett.* 4 (2004) 1755.
- [14] N.V. Gaponenko, I.S. Molchan, O.V. Sergeev, G.E. Thompson, A. Pakes, P. Skeldon, R. Kudrawiec, L. Bryja, J. Misiewicz, J.C. Pivin, B. Hamilton, E.A. Stepanova, *J. Electrochem. Soc.* 149 (2002) H49.
- [15] I.S. Molchan, N.V. Gaponenko, R. Kudrawiec, J. Misiewicz, G.E. Thompson, *Mat. Sci. Eng. B* 105 (2003) 36.
- [16] N.V. Gaponenko, O.V. Sergeev, E.A. Stepanova, V.M. Parkun, A.V. Mudryi, H. Gnaser, J. Misiewicz, R.

- Heiderhoff, L.J. Balk, G.E. Thompson, J. Electrochem. Soc. 148 (2001) H13.
- [17] M. Ishii, S. Komuro, T. Morikawa, J. Appl. Phys. 94 (2003) 3823.
- [18] S. Jeon, P.V. Braun, Chem. Mater. 15 (2003) 1256.
- [19] N. Al Dahoudi, H. Bisht, C. Goebbert, T. Krajewski, M.A. Aegerter, Thin Solid Films 392 (2001) 299.
- [20] I.S. Molchan, N.V. Gaponenko, R. Kudrawiec, J. Misiewicz, G.E. Thompson, P. Skeldon, J. Electrochem. Soc. 151 (2004) H16.
- [21] T. Schuler, M.A. Aegerter, Thin Solid Films 351 (1999) 125.
- [22] M.A. Aegerter, A. Reich, D. Ganz, G. Gasparro, J. Puetz, T. Krajewski, J. Non Cryst. Solids. 218 (1997) 123.